Method For Measuring Sub-Micron Facula At Single-Photon Level With Silicon Photomultiplier

Yaxian Yang
Xi'an Polytechnic University
Guoqing Zhang (zhangg_356@163.com)
Xi'an Polytechnic University
Chen Zhang
Xi'an Polytechnic University
Xinyue Cao
Xi'an Polytechnic University
Lina Liu
Xi'an University of Technology
Lianbi Li
Xi'an Polytechnic University
Xiaoxiang Han
Xi'an Polytechnic University

Research Article

Keywords: Light facula, Silicon Photomultiplier, single-photon, deconvolution, spot size.

Posted Date: November 12th, 2021

DOI: https://doi.org/10.21203/rs.3.rs-1050434/v1

Method for measuring sub-micron facula at single-photon level with Silicon Photomultiplier

Yaxian Yang[1], **Guoqing Zhang**[1,*], **Chen Zhang**[1,+], **Xinyue Cao**[1,+], **Xinyue Cao**[1,+], **Lina Liu**[2,+], **Lianbi Li**[1,+], **and Xiaoxiang Han**[1,+]

[1]School of Science, Xi'an Polytechnic University, 710048, China
[2]School of Science, Xi'an University of Technology, Xi'an, 710048, China
[*]corresponding.author: Email: zhangg_356@163.com
[+]these authors contributed equally to this work

ABSTRACT

Sub-micron faculae (light spots) at the single-photon level have important applications in many fields. This report demonstrates a method for measuring facula size at the sub-micron single-photon level indirectly. The developed method utilizes Silicon Photomultipliers (SiPMs) as the single-photon response detectors, combined with a nano-positioning stage. The approach involves one- or two-dimensional space scanning and a deconvolution operation, which enable evaluations of the size and spatial distribution of focused facula in a single-photon-level pulsed laser. The results indicate that the average full width at half maximum of the faculae is about 0.66 μm, which is close to the nominal resolution of the objective lens of the microscope (0.42 μm). The proposed method has two key advantages: (1) it can measure sub-micron facula at the single-photon level, and (2) the sub-micron facula can easily be aligned with the detector because the array area of the avalanche photodiode cells in SiPM is usually larger than one square millimeter, and there is no need to put an optical slit, knife edge, or pinhole in front of the detector. The method described herein is applicable in weak light facula detection related fields.

Keywords: Light facula; Silicon Photomultiplier; single-photon; deconvolution; spot size.

Introduction

Facula (light spot)-focusing technology has important applications in laser autocollimation and measurements[1], two-dimensional exfoliated materials[2], optical transmission[3], and biological microfluidic tube preparation[4]. These applications require the light beam to be focused on a small facula. Small facula at single-photon level, have important applications in time-dependent fluorescence lifetime spectroscopy[5], confocal laser scanning microscopy (CLSM)[6,7], and single-photon-emission computed tomography (SPECT)[8]. Currently, the conventional method of measuring light faculae includes plate/plane detector measurements[9-11], (slit, aperture, knife port) scanning methods[12-14], and charge coupling device (CCD) imaging[15-17]. Jain et al. [10] used a 194-μm pixel flat panel detector (FPD) combined with a micro pinhole (10 μm) to measure the focal faculae, and they applied a deconvolution method to reduce the fuzzy effect caused by the detector during the measurement process; the size of the measured facula was about 0.6 mm. However, millimeter-level faculae cannot meet the spatial accuracy requirements of many fields and applications[4]. To obtain smaller light faculae, Takeuchi et al.[14] employed a hard X-ray micro-beam edge-scanning system with a multi-pixel detector (CMOS/CCD) and used tantalum film as the edge-pair to scan the focused light beam, thereby improving the knife-edge method; the obtained full width at half maximum (FWHM) of the focused light beam was 25 nm. However, the tantalum Fresnel zone plate (FZP) used in this system was fabricated by a relatively complicated process involving electron beam lithography and reactive ion etching technology. Meanwhile, the CCD imaging method has continued to undergo optimizations. Liu et al.[16] used a CCD to calculate the centroid position of the focal facula based on the two-dimensional (2D) curve of the gray values in the small focal facula; this approach allowed the researchers to measure the size of the light facula with a diameter on the order of dozens of microns. Tiwari et al.[17] situated the CCD photosensitive surface perpendicular to the beam axis, recorded the 2D beam intensity distribution on the

scanning plane via CCD imaging, and measured a facula of 4 μm, which was smaller than the pixel size. For conventional CCD imaging, the size of the photosensitive pixels ranges from several microns to tens of microns (i.e., larger than the light facula at the micron scale), and the pixel gap aberration limits the spatial resolution of light facula measurements [8]. In addition, the CCD used in this method cannot be applied in single-photon detection, which means that it cannot be used to measure a light facula at the single-photon level. To date, measurements of single photons at the sub-micron level has rarely been achieved. Liu [18] used a high-speed rotating hollow probe with a small hole to perform arc scanning in the light field and employed a photomultiplier tube (PMT) as the optical signal detector to measure a Bessel beam with a minimum size of 6 μm. With this method, a non-diffractive light facula with a small energy density and unknown energy distribution could be measured without focusing owing to the high responsiveness, low noise, fast response time, and high quantum efficiency of the PMT. However, the scanning structure was complex, the photon number resolution capability was poor, and the integration level of the system was limited because of the large PMT.

To solve the aforementioned problems, this report proposes a method for measuring sub-micron facula at the single-photon level using a silicon photomultiplier (SiPM), which has recently been applied in many fields and can serve as a substitute for traditional PMT[18-22]. The developed method is used to obtain the one-dimensional (1D) and 2D spatial distributions of the relative photoresponse of SiPM to the light facula by scanning a nano-positioning stage. Then, the 1D and 2D spatial distributions of the relative intensity in light facula under test were determined by a deconvolution operation. No slit, knife edge, or pinhole was required in the developed system.

Experimental setup and principle

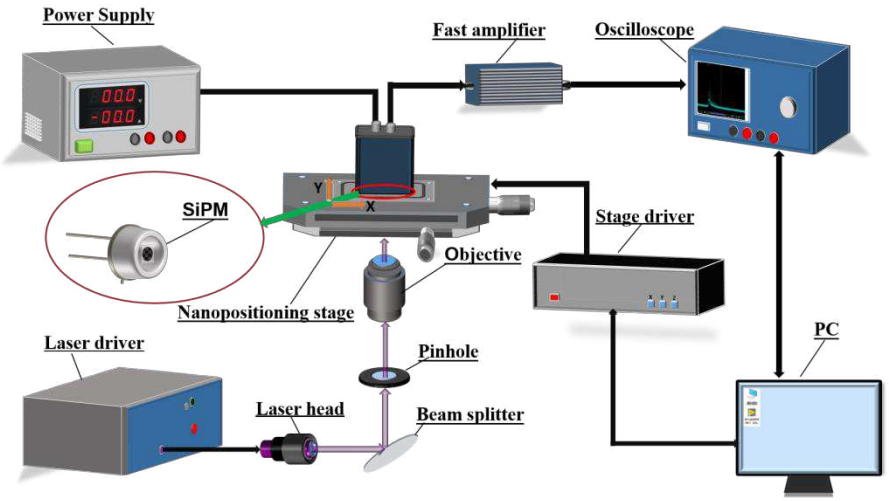

Figure 1. Schematic diagram of the experimental setup for measuring sub-micron light facula at the single-photon level; SiPM = Silicon Photomultiplier; PC = personal computer.

The experimental setup used to measure the sub-micron light faculae is shown in Figure 1. The SiPM was placed in a shielded metal box with light holes, and the photosensitive side of the SiPM was fixed facing downward on the nano-positioning stage (closed-loop displacement accuracy = 2 nm; displacement range = 200 μm; PI nanoXYZ®, Germany), which facilitated alignment with the micro-focused laser facula. The nano-positioning stage driver was controlled by a software program, which could freely move the stage where the SiPM was fixed in the *x*-, *y*-, and *z*-directions. The SiPM was operated in Geiger mode by applying a bias voltage from a power supply. The output avalanche pulse signal was first amplified by the fast amplifier, and then sent into a high-speed digital storage oscilloscope (Tektronix DPO4102B-L digital phosphor oscilloscope; sample rate = 5 GHz; bandwidth = 1 GHz, USA) to record the pulse waveform and pulse counting rate (*PCR*). The threshold of the oscilloscope was set to 0.5 p.e. (where p.e. = photon equivalent) to eliminate the electronic noise from the avalanche pulses. A laser beam generated by a picosecond pulsed laser (PDL-800D; central wavelength = 375 nm; full width at half maximum (FWHM)in the time domain = 44 ps; repetition frequency = 31.125 kHz to 80 MHz; maximum average optical power =

0.7 mW, PicoQuant GmbH Inc. , Germany) was reflected by the beam splitter of the microscope (Olympus X-73, Japan) and passed through a 100-μm pinhole to limit the diameter and intensity of the light beam. Then, the laser beam was focused through the objective lens (Model: LMPLFLN; 100×; resolution = 0.42 μm, Olympus Corp., Japan), thus forming a sub-micron facula on the surface of the SiPM. The intensity of the pulsed laser was adjusted to attenuate the number of photons reaching the photosensitive surface of the SiPM to the single-photon level for each light pulse, which means that there were only a few photons in each laser pulse on average. The relative distance between the SiPM and the objective lens should be optimized for different SiPMs and different times. The SiPM scanned row-by-row by controlling the nano-positioning stage, and the SiPM output pulse counting rate (PCR) at each position in the x- and y-directions was recorded to obtain the data matrix of the PCR. The 1D and 2D PCR distribution maps could then be constructed using any common mathematical software.

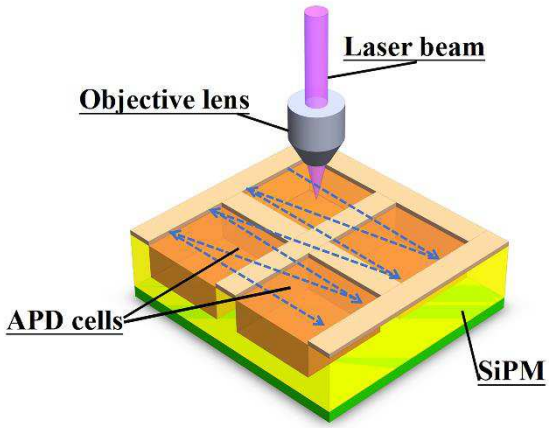

Figure 2. Illustration of the scanning process of the focused laser facula relative to the SiPM (blue dotted lines with arrows represent the scanning route; APD = avalanche photodiode).

A diagram showing the scanning process of the light facula relative to the photosensitive surface of the SiPM is presented in Figure 2. Because the sizes of various SiPMs differ, a suitable scanning step length and number of steps must be set when measuring the *PCR* of an SiPM. The spatial distribution of the *PCR* can also be called the spatial distribution of the detector's relative photoresponse because the *PCR* directly reflects the local relative light response of the detector. The intensity of the laser pulse remained constant during the experiment, so the spatial distribution of the intensity of the focused laser facula reaching different SiPM surfaces should also be constant. If the size and shape of the SiPM's photosensitive region and the spatial distribution of its photoresponse are known, the intensity distribution and size of the facula can be deduced by a deconvolution method. The spatial 1D and 2D distributions of the relative light intensity in a focused laser facula can be obtained by deconvoluting the 1D and 2D spatial distribution data (vide infra and Figure 3) of the relative photoresponse of the SiPM based on the shape of its photosensitive region.

An SiPM is composed of avalanche photodiode (APD) cells with a regular shape (most are square) and gaps between adjacent APD cells. The measured 2D relative photoresponse data h(x,y) can be regarded as the convolution of a rectangular function g(x,y) and the spatial distribution function of the laser facula intensity *f*(*x*,*y*), which are related through the expression in equation (1),

$$f(x, y) * g(x, y) + \varepsilon(x, y) = h(x, y) \quad (1)$$

where *x* and *y* are the coordinates in the waist cross-section of the focused laser beam perpendicular to the propagation direction of the beam, and ε(x,y) is the noise fluctuation of the measured signal, which can be eliminated by a low-pass filtering operation. Then, the intensity distribution function *f*(*x*,*y*) can be obtained via deconvolution. Take the discrete Fourier transformation of *h*(x,y) and *g*(x,y) in equation (2) and (3), respectively,

$$H(f_x, f_y) = \int_{-L_0/2}^{L_0/2} h(x, y) e^{i2\pi(f_x x + f_y y)} \mathrm{d}x\mathrm{d}y \tag{2}$$

$$G(f_x, f_y) = \int_{-L_0/2}^{L_0/2} g(x, y) e^{i2\pi(f_x x + f_y y)} dxdy \tag{3}$$

where L_0 is the scanning range. Then, according to the Fourier transformation principle, we can define the relationship in equation (4),

$$F(f_x, f_y) = H(f_x, f_y) / G(f_x, f_y) \tag{4}$$

where $F(f_x,f_y)$ is the Fourier transformation of $f(x,y)$. The spatial distribution function of the relative light intensity in the focused laser facula f(x,y) can then be obtained by the inverse Fourier transformation, as shown in equation (5):

$$f(x, y) = F^{-1}\{F(f_x, f_y)\} \tag{5}$$

The size of the focused laser facula can be estimated by eye in the map of $f(x,y)$, while a more precise size (defined as the FWHM) of the focused laser facula can be obtained through function fitting of $f(x,y)$. For the 1D relative light intensity distribution of a light facula, $f(x)$ or $f(y)$ can be obtained by fixing the x- or y-coordinate during the deconvolution operation described above. Similarly, the facula size along the x- or y-direction can be obtained through unary function fitting of $f(x)$ or $f(y)$, respectively. The output beam from the semiconductor laser was used in the fundamental mode, so it was a Gaussian beam, which was focused to a Bessel beam by the lens along its longitudinal axis . According to the well-known principle of optics [23], $f(x)$ or $f(y)$ can be fitted by the Airy formula based on the Bessel function, as shown in equation (6),

$$I(v) = \left[\frac{2J_1(v)}{v}\right]^2 I_0 \tag{6}$$

where $I(v)$ is the intensity distribution of a light facula, v is the distance relative to the extreme point of the distribution, $J_1(v)$ is the first-order Bessel function in the first class, and I_0 is the maximum intensity of the distribution. Because the measured relative photoresponse data includes the dark count rate of the SiPM and possible stray-photon-induced pulse counts, an intensity shift should be integrated into the fit function, as shown in equation (7),

$$I(v) = \left[\frac{2J_1(v)}{v}\right]^2 I_0 + I_d \tag{7}$$

where I_d is the baseline of the light intensity distribution.

Experimental results and analysis

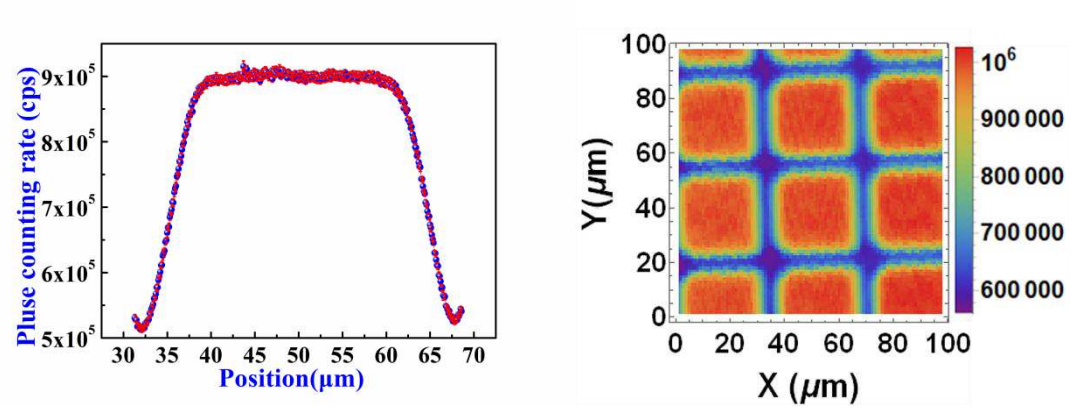

(a) (b)

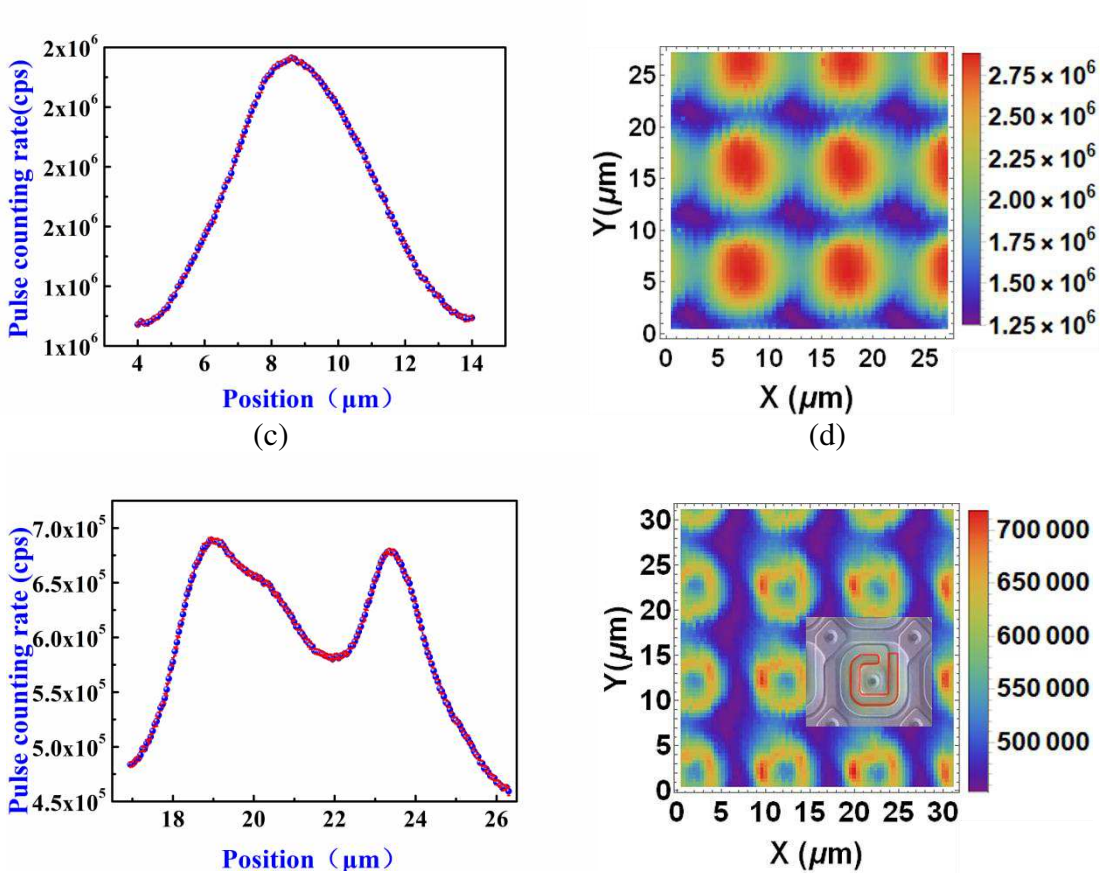

Figure 3. Spatial 1D and 2D distributions of the relative photoresponse (PCR recorded at 0.5 p.e. threshold) of SiPMs to single-photon-level light facula. (a) 1D and (b) 2D distribution of the PCR of the SiPM from Fondazione Bruno Kessler (FBK), Italy (model = LF-HD), with 35 μm APD cell pitch; (c) 1D and (d) 2D distribution of the PCR of the SiPM from novel device laboratory(NDL),China (model = EQR1011-1010C-T), with 10 μm APD cell pitch; (e) 1D and (f) 2D distribution of the PCR of the Hamamatsu SiPM (model = S12571-010C) with 10 μm APD cell pitch.

From **Error! Reference source not found.**a and 3b, it is clear that the spatial distribution of the relative photoresponse within an APD cell is uniform, and different APD cells can be easily distinguished. Since the gap size between the 35 μm APD cells of the FBK SiPM is 5 μm, it can be concluded that the FWHM of the facula is significantly smaller than 5 μm. If the facula size is larger than 5 μm, different APD cells would not be distinguishable. Similarly, **Error! Reference source not found.**c and 3d show the 1D and 2D distributions, respectively, of the relative photoresponse of the NDL SiPM (APD cell pitch = 10 μm), wherein the side length of the APD photosensitive region is 7 μm, and the size of the gap between two neighboring APD cells is 3 μm. In this case, the APDs are still distinguishable, indicating that the size of the facula is smaller than 3 μm. Finally, Figure 3e and 3f show the 1D and 2D distributions, respectively, of the relative photoresponse of the Hamamatsu SiPM with a 10-μm APD cell pitch. The details in each APD cell can still be resolved by eye (Figure 3f), and the inset in Figure 3f shows the electron micrograph of the 10-μm APD cell. The region surrounded by the red solid line in the inset is the un-shading region surrounded by quenching resistor film; this region forms a square ring with a width of approximately 1 μm. The square ring-shaped photosensitive region is relatively clearly resolved (Figure 3f), which indicates that the FWHM of the light facula should be smaller than 1 μm.

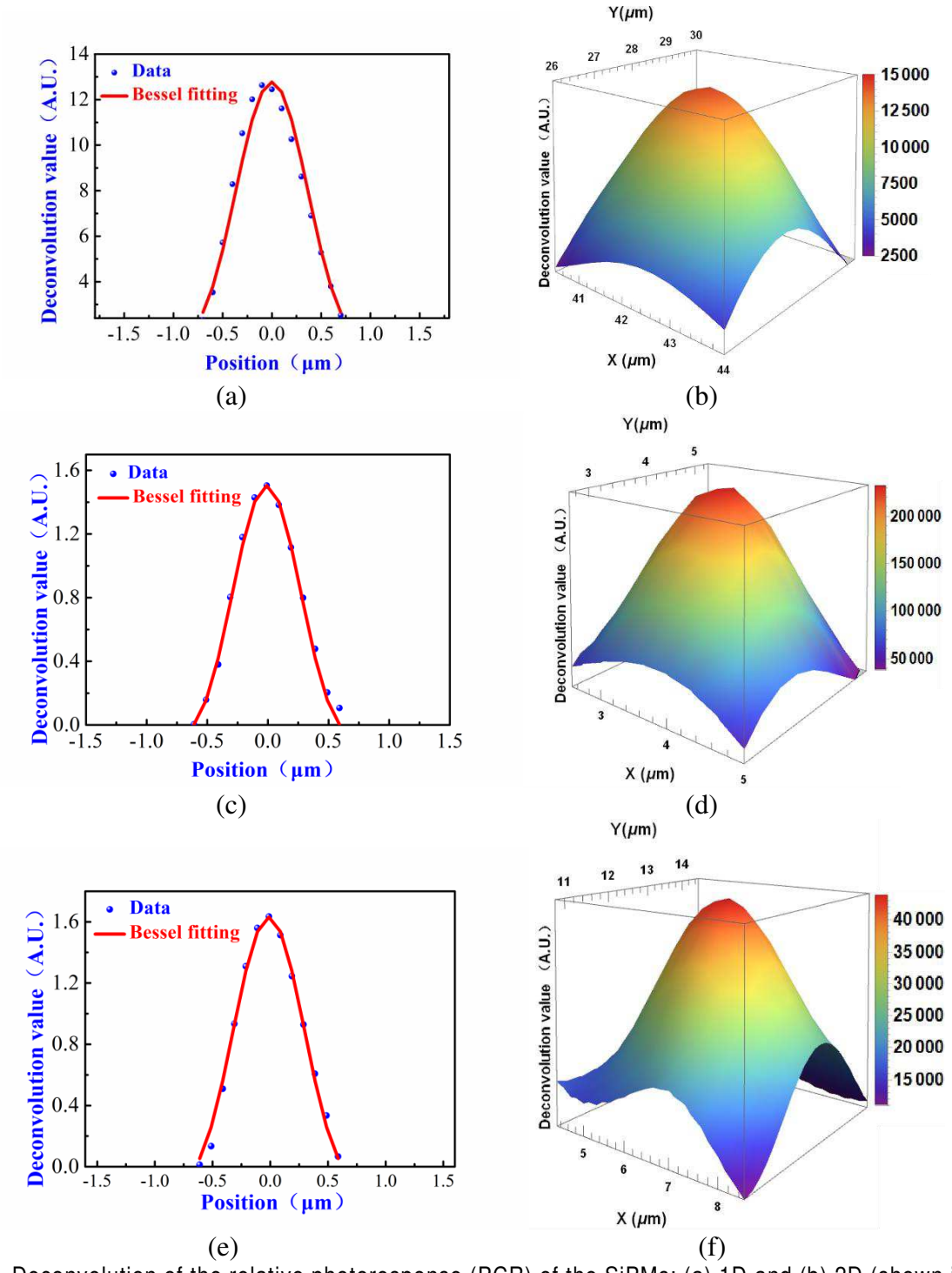

Figure 4. Deconvolution of the relative photoresponse (PCR) of the SiPMs: (a) 1D and (b) 2D (shown in 3D-view) deconvolution values obtained for the FBK SiPM with 35 μm APD cell pitch (model = LF-HD); (c) 1D and (d) 2D (shown in 3D-view) deconvolution values obtained for the NDL SiPM with 10 μm APD cell pitch (model = EQR1011-1010C-T); (e) 1D and (f) 2D (shown in 3D-view) deconvolution values obtained for the Hamamatsu SiPM with 10 μm APD cell pitch (model = S12571-010C).

The 1D deconvolution results (Figure 4) of the 1D spatial distributions of the PCR of SiPMs (Figure 3) were obtained according to equation (1–5). It is clear that for each of the tested SiPMs, the spatial distribution range of light facula intensity was on the micron scale, and the intensity distribution of the laser facula closely followed a Bessel distribution. To quantitatively evaluate the size of the laser faculae, the Airy formula based on the Bessel function (equation (7)) was used to fit the 1D deconvolution results. The

fitting results are shown as solid red lines in Fig.4a, 4c, and 4e, and the fitting parameters are presented in Table 1 The fitting results indicated that the average FWHM of the laser faculae was 0.66 μm. To intuitively visualize the relative intensity distributions of the laser faculae, the 2D deconvolution operation was performed with the data shown in Figure 3b, 3d, and 3f to obtain the 3D views of the deconvolution results (shown in Figure 4b, 4d, and 4f, respectively). The spatial distribution range of the light facula under test was basically consistent with the 1D results.

Table 1. Fitting parameters of the light facula under test

Model	APD cell pitch	FWHM of the laser facula (μm)	Adjusted R^2
NDL SiPM (EQR1011-1010C-T)	10 × 10 μm	0.64	0.997
FBK SiPM (LF-HD)	35 × 35 μm	0.68	0.996
Hamamatsu(S12571-010C)	10 × 10 μm	0.65	0.995

Table 1 shows the FWHM of focused laser facula measured by the three models of SiPMs; these results are generally consistent with the nominal resolution of the objective lens of the microscope (i.e., 0.42 μm) and with the focused facula size (i.e., 0.8 μm) mentioned by Anfimov et al. [24] when measuring the fill factor of a SiPM via focused laser scanning. It is worth noting that the obtained results are 36% larger than the nominal facula resolution of the objective lens (0.42 μm), which may be due to the fact that the setup of the optical path was not adjusted to the optimal state. Additionally, the adjusted R2 coefficients are all close to 1, indicating that the light intensity distribution of the laser facula follows a Bessel distribution with high confidence. Therefore, the facula size evaluation results obtained in these experiments were reasonable.

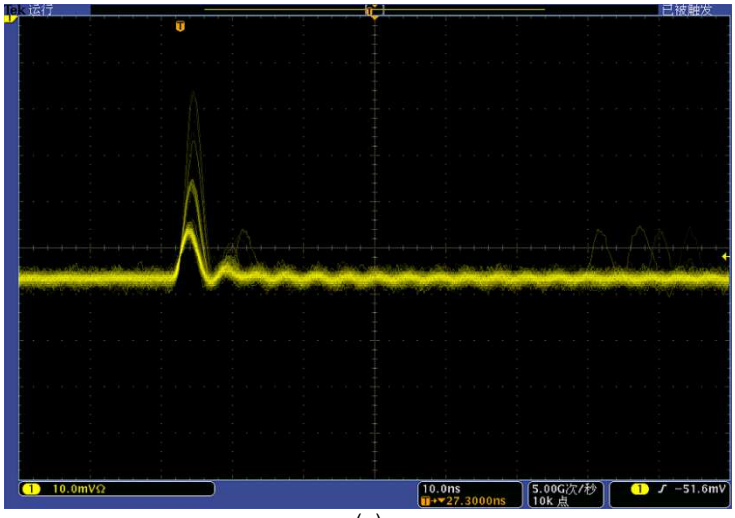

(a)

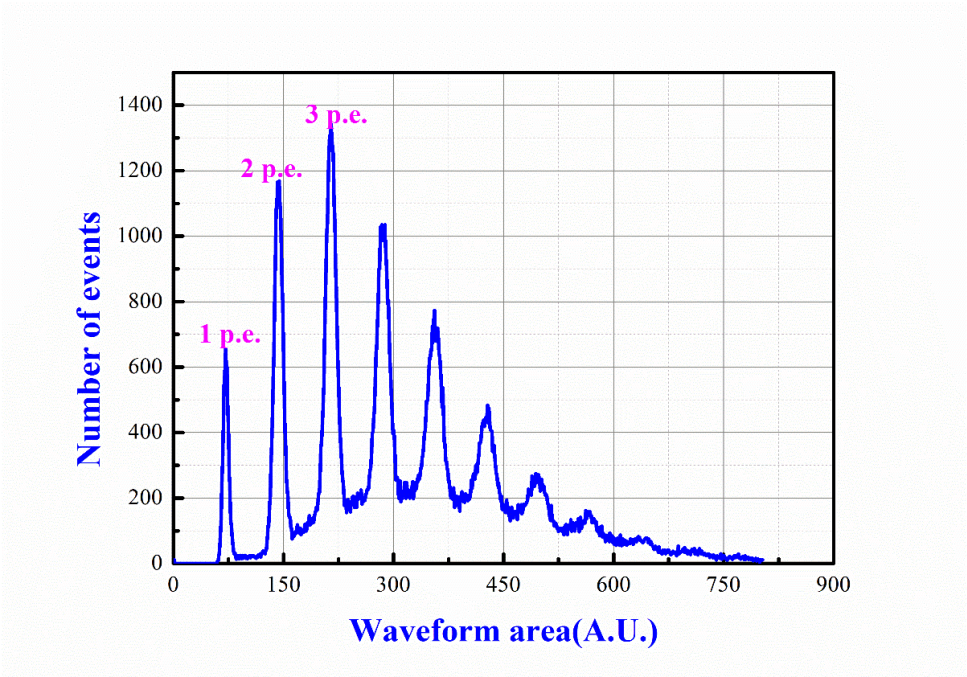

(b)

Figure 5. (a) Oscillograph showing the avalanche pulses from the SiPM under the irradiation of a focused laser facula; (b) photon number resolution (pulse height distribution) spectrum of the Hamamatsu SiPM (model = S12571-010C).

To confirm that the light facula incident on the detector is weak to the single-photon level, we recorded the oscilloscope capture and measured the pulse height distribution spectrum of the avalanche pulses output by the Hamamatsu SiPM with 10 μm APD cell pitch (Figure 5). Single-photon response pulses were clearly observed, and the pulses has a clear multiple relationship, corresponding to the number of detected photons (see Figure 5a). Additionally, Figure 5b shows a clear discrete photon-equivalent peak, which indicates that the most probable number of detected photons is 3. Since the discrete peaks in Figure 5b correspond to the number of detected photons, this plot is often called the photon number resolution spectrum. Overall, the results in Figure 5 confirm that the number of photons hitting the SiPM is at single-photon level.

Conclusions

It has been verified that an SiPM combined with precision scanning can be used to indirectly measure the size of a sub-micron light facula at the single-photon level. According to the deconvolution results from the measured 1D relative photoresponse distribution data, the average FWHM of the evaluated facula was about 0.66 μm, which is close to the resolution of the objective lens in the microscope (0.42 μm). The proposed method has two key advantages: first, it can be used to measure a sub-micron facula at the single-photon level, and second, the light facula can easily be aligned with the detector. Through rapid scanning and a deconvolution operation, the spatial distribution of the intensity in a light facula can be obtained, which could lead to various applications in weak light facula detection and the development of sub-micron facula measurement techniques.

Acknowledgements

This work was supported by the National Natural Science Foundation of China (Grant Nos. 11975176), the Natural Science Basic Research Plan in Shaanxi Province of China (Grant No. 2019JM-139), the Key Research and Development Program of Shaanxi Province (Grant No. 2020KW-011), and Science and Technology Plan Project of Xi'an (Grant No. 2020KJRC0026).

Author contributions statement

Yaxian Yang wrote the main manuscript text and analysed the results, Guoqing Zhang proposed the main ideas and overall planning, Chen Zhang and Xinyue Cao conducted some experiment(s), Lina Liu built the main experimental setup, Lianbi Li give some support for building the experimental setup, Xiaoxiang Han amended and checked the whole paper. All authors reviewed the manuscript.

References

1 Y. Shimizu, etal. Ultra-sensitive angle sensor based on laser autocollimation for measurement of stage tilt motions. *Optics Express*. 24, 2788-2805, DOI:https://doi.org/10.1364/OE.24.002788 (2016).

2 Y. Mao, etal. A vacuum ultraviolet laser with a submicrometer facula for spatially resolved photoemission spectroscopy. *Light: Science & Applications*.10, 22-30, DOI: https://doi.org/10.1038/s41377-021-00463-310(1), (2021).

3 M. Aiba, B. Beutner, N. Milas, Beam-size-free optics determination. *Nuclear Instruments and Methods in Physics Research.* 753, 24-33,DOI: http://dx.doi.org/10.1016/j.nima.2014.03.031 (2014).

4 L. Yang, S. Ji, K. Xie, W. Du, B. Liu, High efficiency fabrication of complex microtube arrays by scanning focused femtosecond laser Bessel beam for trapping/releasing biological cells. *Optics Express*. 25, 8144-8157,DOI:https://doi.org/10.1364/OE.25.008144 (2017).

5 K. Suhling etal. Fluorescence lifetime imaging (FLIM): Basic concepts and some recent developments. *Medical Photonics*. 27, 3-40 ,DOI:http://dx.doi.org/10.1016/j.medpho.2014.12.001(2015) .

6 L. Thibon, L. E. Lorenzo, M. Piché, Y. D. Koninck, Resolution enhancement in confocal microscopy using Bessel-Gauss beams. *Optics Express*. 25, 2162-2177, DOI:https://doi.org/10.1364/OE.25.002162 (2017).

7 E. Slenders, M. Castello, M. Buttafava, F. Villa, G. Vicidomini, Confocal-based fluorescence fluctuation spectroscopy with a SPAD array detector, *Light: Science & Application*s. 10, 31-42, DOI:https://doi.org/10.1038/s41377-021-00475-z (2021).

8 T. A. Holly, B. G. Abbott, M. Al-Mallah, D. A. Calnon, P. Soman, Single photon-emission computed tomography. *Journal of Nuclear Cardiology*. 17, 941-973, DOI:https://doi.org/10.1007/s12350-010-9246-y(2010).

9 X. Wang, X. Su, G. Liu, J. Han, R. Wang, Investigation of high-precision algorithm for the facula position detection for four-quadrant detector. *Optik*. 203, 163941,DOI:https://doi.org/10.1016/j.ijleo.2019.163941(2019) .

10 A. Jain, A. Panse, D. R. Bednarek, S. Rudin, Focal facula measurements using a digital flat panel detector. Spie Medical Imaging. 9033, (90335F); 10.1117/12.2043057(2014).

11 B. Wu, L. G. Li, S. Q. Liu, C. P. Ying, K. F. Chen, Accurate focusing of knife-edge imaging optical system based on the area under MTF curve. *Proceedings of SPIE - The International Society for Optical Engineering*. 8908, 89081U-89081U-6;10.1117/12.2034545(2013) .

12 G. Anoop, T. D. Milster, Spot distribution measurement using a scanning nanoslit. Applied Optics. 50, 4746-54, 10.1364/AO.50.004746(2011) .

13 M. González-Cardel, P. Arguijo, R. Díaz-Uribe, Gaussian beam radius measurement with a knife-edge: a polynomial approximation to the inverse error function. *Applied Optics*. 52, 3849-3844,DOI:http://dx.doi.org/10.1364/AO.52.003849 (2011).

14 A. Takeuchi, Y. Suzuki, K. Uesugi, Differential-phase-contrast knife-edge scan method for precise evaluation of X-ray nanobeam, *Japanese Journal of Applied Physics*. 54, 092401 DOI:http://dx.doi.org/10.7567/JJAP.54.092401(2015).

15 L. G. Sheng, Y. Lv, L. S. Liu, R. Geng, X. Y. Li, A High Accuracy Sub-Pixel Light facula Positioning Algorithm. *Applied Mechanics and Materials*. 644-650, 1459-1463, DOI:https://doi.org/10.4028/www.scientific.net/AMM.644-650.1459(2014).

16 X. Liu, Z. Lu, X. Wang, D. Ba, C. Zhu, Micrometer accuracy method for small-scale laser focal facula centroid measurement. *Optics & Laser Technology.* 66, 58-62, DOI:http://dx.doi.org/10.1016/j.optlastec.2014.07.016(2015).

17 S. K. Tiwari, S. P. Ram, J. Jayabalan, S. R. Mishra, Measuring a narrow Bessel beam facula by scanning a charge-coupled device (CCD) pixel. *Measurement Science and Technology*. 21, 025308, DOI:http://iopscience.iop.org/0957-0233/21/2/025308(2010) .

18 Y. Liu, B Zhao. Scanning method is used to measure the energy distribution of non-diffraction imaging microspots. *Applied Optics*. 06, 11-14; CNKI:SUN:YYGX.0.2007-06-004(2007). (in Chinese)

19 K. Yamamoto, T. Nagano, R. Yamada, T. Ito, Y. Ohashi, Recent Development of MPPC at Hamamatsu for Photon Counting Applications, *Proceedings of the 5th International Workshop on New Photon-Detectors,* (PD18), DOI:https://doi.org/10.7566/JPSCP.27.011001(2019).

20 F. Acerbi, S. Gundacker, Understanding and simulating SiPMs, *Nuclear Instruments and Methods in Physics Research*. 926,16-35, DOI:https://doi.org/10.1016/j.nima.2018.11.118(2019).

21 A. Nagai , etal. Characterization of a large area silicon photomultiplier, Nuclear Instruments and Methods in Physics Research. 948, DOI:https://doi.org/10.1016/j.nima.2019.162796(2019).

22 A. Vacheret ,et al. Characterization and simulation of the response of Multi-Pixel Photon Counters to low light levels. *Nuclear Instruments and Methods in Physics Research*. 656, 69-83, DOI:https://doi.org/10.1016/j.nima.2019.162796(2011).

23 Born.M. Wolf.E. Principles of optics. 180-181 (Publishing House Of Electronics Industry, 1980).

24 N. V. Anfimov, V. Vorobel, Y. S. Kovalev, P. Kodyš, Scanning a Silicon Photomultiplier with a Laser Beam. *Physics*

of Particles and Nuclei Letters. 16, 820-825; 10.1134/S1547477119060025(2019)